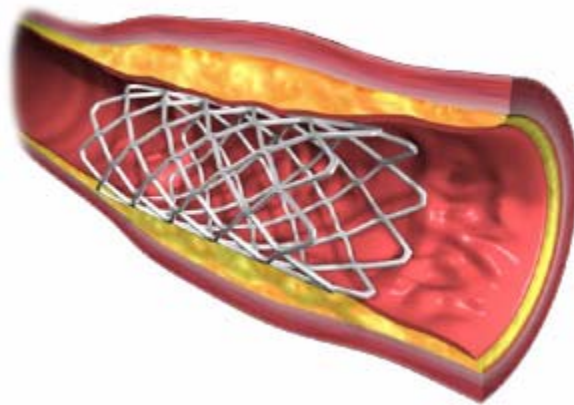


# **Drug-Eluting Stents: Design for Prevention of Angioplastic Restenosis**



Bonnie Chen  
Nisse Clark  
Molly Melhem  
Gwen Owens

BEE 453: Computer-Aided Engineering  
Professor Ashim K. Datta  
Spring 2006

# Table of Contents

[1] Executive Summary.....	3
[2] Introduction and Design Objectives.....	3-5
2.1 Introduction.....	3-4
2.2 Problem Schematic.....	4-5
2.3 Objectives.....	5
[3] Results and Discussion.....	5-12
3.1 Major Findings.....	5-9
3.2 Sensitivity Analysis.....	9-12
3.3 Results vs. Expected Results.....	12
[4] Conclusions and Design Recommendations.....	13-14
4.1 Conclusion.....	13
4.2 Realistic Constraints.....	13
4.3 Design Recommendations.....	14
[5] Appendices.....	14-26
Appendix A.....	14-17
A.1 Geometry and Schematic.....	14-15
A.2 Input Parameters.....	15-16
A.3 Initial and Boundary Conditions.....	16-17
Appendix B.....	17-22
B.1 Solver Statements.....	17-19
B.2 Mesh Convergence.....	19-21
B.3 FIINP File.....	21-22
Appendix C.....	22-25
Appendix D.....	26

## **[1] Executive summary**

Balloon angioplasty and coronary stent deployment are powerful techniques in the treatment of individuals with advanced coronary artery disease. Recent advancements have led to the development of drug-eluting stents designed to release a drug polymer that inhibits restenosis, a bodily defense mechanism characterized by tissue ingrowth and reblockage of the artery. The stent is coated with an anti-cancer or immunosuppressive drug that diffuses through the surrounding tissues over a critical period of time. In this study, diffusion of the drug Rapamycin was modeled using computer-aided design software. Analysis was performed in order to determine the concentration profile of the drug at various time intervals. The stent geometry was reduced to six concentric rings of 1.5 mm width spaced 1.5 mm apart, resulting in a total stent length of 16.5 mm. Diffusion was modeled from only one of these rings and conclusions were drawn considering the global diffusion from multiple rings of this type. A graded mesh was generated in GAMBIT, and simulations were executed in FIDAP to assess the drug concentration as a function of several input parameters. It was concluded that the drug reaches  $48 \mu\text{g}/\text{m}^3$ , within a defined therapeutic concentration range of  $40\text{-}60 \mu\text{g}/\text{m}^3$ , after about nine months at a penetration depth of 0.015 mm. This indicates that after nine months the first tissue layer surrounding the coronary lumen, also known as the intima, is saturated with drug at concentrations necessary for the prevention of restenosis. Sensitivity analysis was performed to test the stability of our solution and to assess factors which may affect the diffusion process. It was found that the concentration of Rapamycin was most sensitive to a change in diffusivity of Rapamycin in the intimal tissue layer, whereas the drug concentration was less sensitive to changes in the stent diffusivity and variance in initial concentration of drug immobilized in the stent.

## **[2] Introduction and Design Objectives**

### **2.1 Introduction**

Coronary artery disease is a result of plaque buildup on the interior walls of arteries that supply blood to the heart. As buildup increases, the area within the artery that allows for blood flow decreases. The decrease in flow allows clots to form on the surface of the wall and leads to, in the majority of cases, a heart attack. Risk factors for this disease include, but are not limited to, smoking, high blood pressure, high cholesterol, diabetes, obesity and physical inactivity. Coronary artery disease is the most common heart disease and the leading cause of death in the United States and can be attributed to over 500,000 deaths a year and thus should not be taken lightly.

Methods to treat coronary artery disease focus on widening the flow area of the artery by pushing the plaque towards the arterial walls. The first procedure was performed in 1977 and involved a balloon catheter that was navigated into the affected artery through a small incision in the leg or the arm of the patient. Once the destination was reached, the doctor would then inflate the balloon to widen the artery. This procedure would relieve the patient of the chest pain for several months, but over 30% of all coronary arteries would begin to close up again, a phenomenon known as restenosis. Once restenosis has occurred, the patient would either find

himself in the same situation as before the procedure or have to endure an emergency bypass graft surgery, depending on the amount of time that has elapsed since the initial surgery.

In 1986 the metal stent was introduced to help lower the rate of restenosis in balloon angioplasty patients. Coronary stents are cylinders made of metal mesh that is almost analogous to a metal fence. They are placed on a separate balloon catheter that is inserted after the first balloon angioplasty. Once the artery is widened by the first procedure, the balloon catheter containing the stent is inserted and opened at the location of the plaque buildup. With this stent in place it was believed that the artery would remain widened, however, restenosis still occurred in 25% of the cases, resulting in a necessity of a repeat procedure. It was through investigating the restenosis that occurred after stent injection that doctors concluded that restenosis was not just a second buildup of plaque, but rather scar tissue formation after angioplasty. In the specific case of the metal stent, the body responded to the foreign object by treating it as a wound and as an outcome scar tissue grows around the metal and into the artery. The physicians could now use this information to help battle restenosis through a variety of different methods with one of the more successful ones being drug delivery by the stent itself.

Drug-eluting stents are coated with a drug that interrupts the restenosis process. By placing this stent into the body, it not only opens the artery, but also prevents the scar-tissue formation that occurs concurrently with angioplasty. This is a fairly new procedure with the first FDA approval on April 24, 2003, however the results of recent studies look promising. Out of 1,000 patients that were enrolled in a study, only 3.9% in the drug coated group experienced restenosis, compared to 35.4% that were given the bare metal stents.

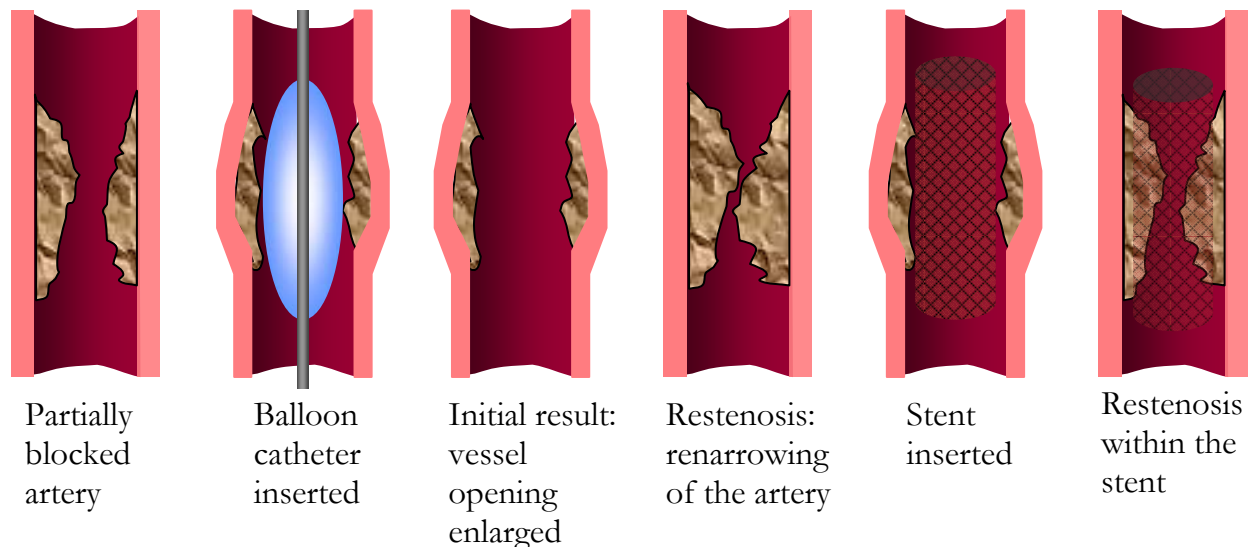


**Figure 2.1:** This is an illustration of an angioplasty procedure and the results obtained with a stent that does not elute drugs. Without a drug-eluting stent, restenosis was found to occur by building plaque back up within the spaces of the stent, thus, resulting in a need for a drug to prevent restenosis.

## 2.2 Problem Schematic

The coronary artery was modeled as having a stent embedded in two tissue layers: intima and adventitia. The stent geometry was simplified to six concentric rings with a square-cross section. Each ring was 1.5 mm in width and spaced 1.5 mm apart (see Appendix A). A total of six rings were used to model an actual stent of length 16.5 mm. Diffusion was only modeled from one of

these rings and the final solution was multiplied to include the global diffusion from all six rings. The coronary artery was modeled as a right cylindrical element with concentric rings that were axi-symmetric about the center lumen. As shown in Appendix A.1.1, the problem contained three regions: the stent region, the intima region and the adventitia region. The lumen was excluded from the geometry. Instead, a convective term was specified at the lumen-intima/stent interface to mimic blood flow. The problem was transient with an initial concentration at the stent and a convection term due to blood flow at the lumen interface. See Appendix A for the governing equation, boundary and initial conditions.

## 2.3 Objectives

By modeling the interaction of the drugs in the stent with the tissue in the artery, we wanted to accurately model and determine the time at which a steady-state concentration was reached and the time at which a therapeutic concentration was maintained in the intima. An additional objective was to determine the sensitivity of the concentration of Rapamycin in the intima to varying parameters, as discussed in the sensitivity analysis. Additionally, accurately modeling a complex biomedical physical situation within the constraints of Fidap and Gambit was a main objective.

# [3] Results and Discussion

## 3.1 Major Findings

The simulation was run at time intervals of 1 day, 1 week, 1 month, 2 months, 6 months, and 2 years to evaluate solution convergence. Contour plots are shown in Figure 3.1 and 3.2; a corresponding graph of the concentration versus time is shown in Figure 3.3. From these figures it can be seen that the solution converges just before time = 25,000,000 seconds. This is equivalent to about 9 months. Our goal was to find the time at which a therapeutic concentration range of 40-60  $\mu\text{g}/\text{m}^3$  was reached at the intima/adventitia interface above the center of the stent (concentration plots were derived for the node at  $x = 0$  and  $y = 1.53 \text{ mm}$ )<sup>7</sup>. We made the assumption that the entire intima had to be at a therapeutic concentration in order to prevent restenosis. Also, assuming that each concentric ring was spaced a distance of one ring width apart, the entire intima would be saturated with therapeutic drug concentration when node (0,1.53) was saturated. Figure 3.3 shows that a single ring reaches a drug concentration of about 8  $\mu\text{g}/\text{m}^3$  after this time. Considering the cumulative effect of all six rings, the intima is saturated with a total concentration of 48  $\mu\text{g}/\text{m}^3$  after nine months. This value is within the range of our therapeutic concentration. It is thus concluded that a Rapamycin-eluting stent of diffusivity  $D = 1 \times 10^{-13} \text{ m}^2/\text{s}$  and initial drug concentration  $c_s = 170 \mu\text{g}/\text{m}^3$  will generate a sufficient amount of medication to prevent restenosis in a period slightly less than a year. All properties, boundary conditions, initial conditions, governing equations are stated in Appendix A.

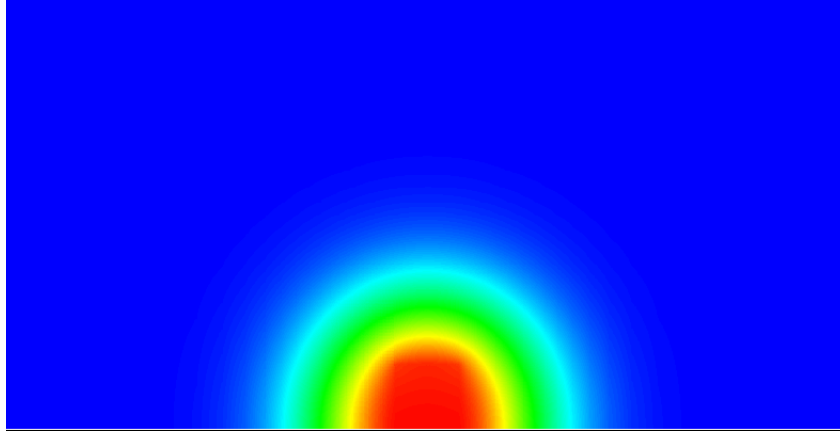


**Figure 3.1:** A contour plot of the entire geometry after the solution has converged in less than a year. Regions far from the stent show a zero concentration (royal blue). This means that our simplified geometry was large enough to encompass the regions of changing concentration. From this contour plot, it is apparent that we could reduce the geometry size further in an attempt to decrease the computing time.

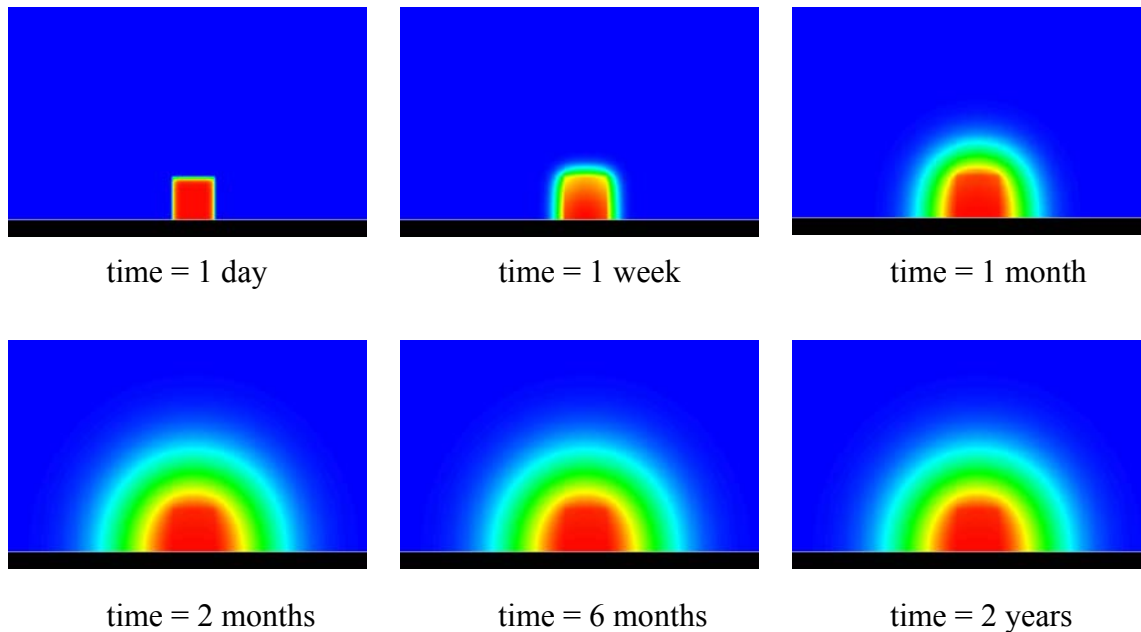


**Figure 3.2:** Contour plots of the drug concentration for varying time intervals of time = 1 day, 1 week, 1 month, 2 months, 6 months, and 2 years. The contour regions shown are for a reduced geometry emphasizing the regions of greatest concentration gradients. After 6 months it is evident that the concentration profile has almost reached a steady state as it is very similar to the contour plot for time = 2 years.

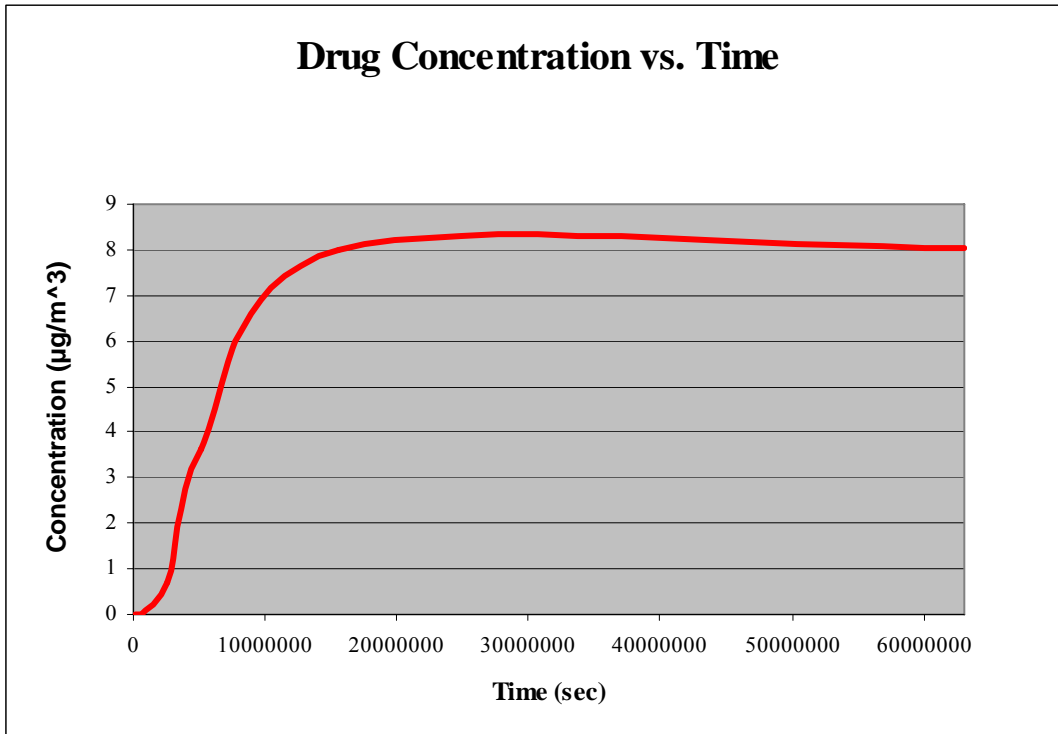


**Figure 3.3:** Concentration plot of the drug concentration for a node taken at the intima/adventitia interface. The drug concentration is shown to converge after a time of about 9 months. The final concentration at the plotted node is about  $8 \mu\text{g}/\text{m}^3$  for a single ring. This means that a total concentration of  $6 \times 8 \mu\text{g}/\text{m}^3 = 48 \mu\text{g}/\text{m}^3$  is in the arterial region after 9 months. An initial drug concentration of  $170 \mu\text{g}/\text{m}^3$  in the stent was used.

The contour plot is as expected, with uniform diffusion of the drug from the highest concentration region in the stent diffusing into the tissues. Our assumption of a square cross section of the ring element does not matter because the concentration profile assumes a radial distribution as the solution converges over time. The concentration plot is also as expected. Rapid concentration gradients occur during the first few months following stent implantation. In fact, a linear region exists before time = 10,000,000 seconds, or during the first four months. From then on, the concentration is increasing in the tissues at a decreasing rate. It is not until nine months that the drug has reached its maximum concentration within the tissue regions. This model does not take into account the degradation of the drug over time because the complexity of Rapamycin pharmacokinetics have made studies on degradation rates for long time periods relative unfeasible. After nine months, the drug concentration will decrease but restenosis will still have been prevented. This is assumed because the drug was at an optimum concentration during the critical time at which restenosis is likely to occur.

Figure 3.4 shows the concentration plot for several randomized nodes over time. This graph further demonstrates that a solution is converging after a non-dimensionalized time of 5. This is equivalent to slightly less than a year, as expected. Figure 3.5 shows a similar concentration plot for several different nodes within the adventitia region. The bluer lines toward the top of the graph are closet to the stent. Subsequent lines show nodal concentrations at linearly increasing distances from the stent, showing that concentrations were smaller further from the drug source.





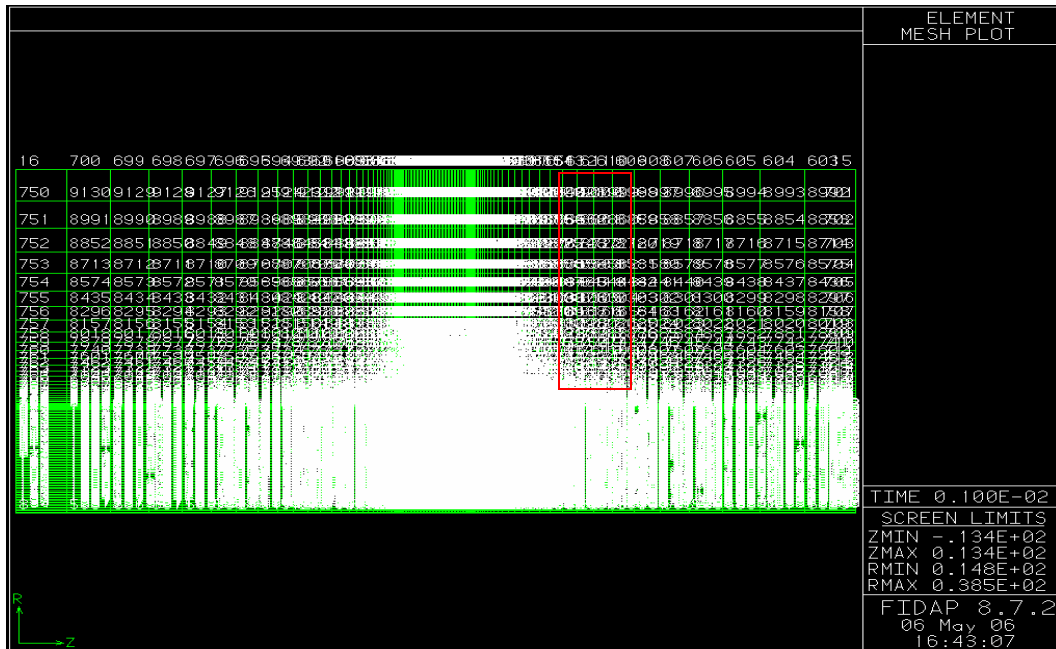


**Figure 3.6:** The region of nodes for Figure 3.5 were picked from the highlighted region, which consists of the adventitia tissue. Nodes closest to the stent had higher concentrations of Rapamycin, as seen in Figure 3.5.

### 3.2 Sensitivity Analysis

Because drug-eluting stents are complex implanted medical devices, simulation of the elution of Rapamycin is influenced by many factors, such as geometry of the stent, diffusion through heterogeneous materials, and chemical properties of the released drug. In order to determine the validity of our solution and the potential range of results that could be obtained by varying input parameters, we performed sensitivity analysis for variations in initial drug concentration, diffusivity, and reaction rate, all of which are relevant for effective stent design. Large variations were found for each parameter in the literature; this was further analyzed in Appendix C. For our analysis of the solution sensitivity to various parameters, it was assumed that a maximum of 20% error was inherent in the values used in the final solution.

#### 3.2.1 Variation of Initial Concentration of Rapamycin in Stent

Sensitivity analysis was performed on initial drug concentration because wide variation in drug concentration was found in manufactured drug-eluting stents due to differences in a) stent length based on medical necessity due to initial area of arteriolar blockage, b) stent radius based on the gender and age of the angioplasty patient, and c) nature of the anti-restinosis drug based on variable therapeutic and toxic concentrations. For our simulation, the initial, homogenous concentration of Rapamycin in the stent was assumed to be  $170 \mu\text{g}/\text{m}^3$ .<sup>7</sup> Figure 3.7 shows that varying the initial concentration of Rapamycin in the stent yielded a variation in concentration in the intima of +10.5% to -8.5%. Therefore, the simulation is moderately sensitive to the initial concentration of Rapamycin immobilized in the stent.

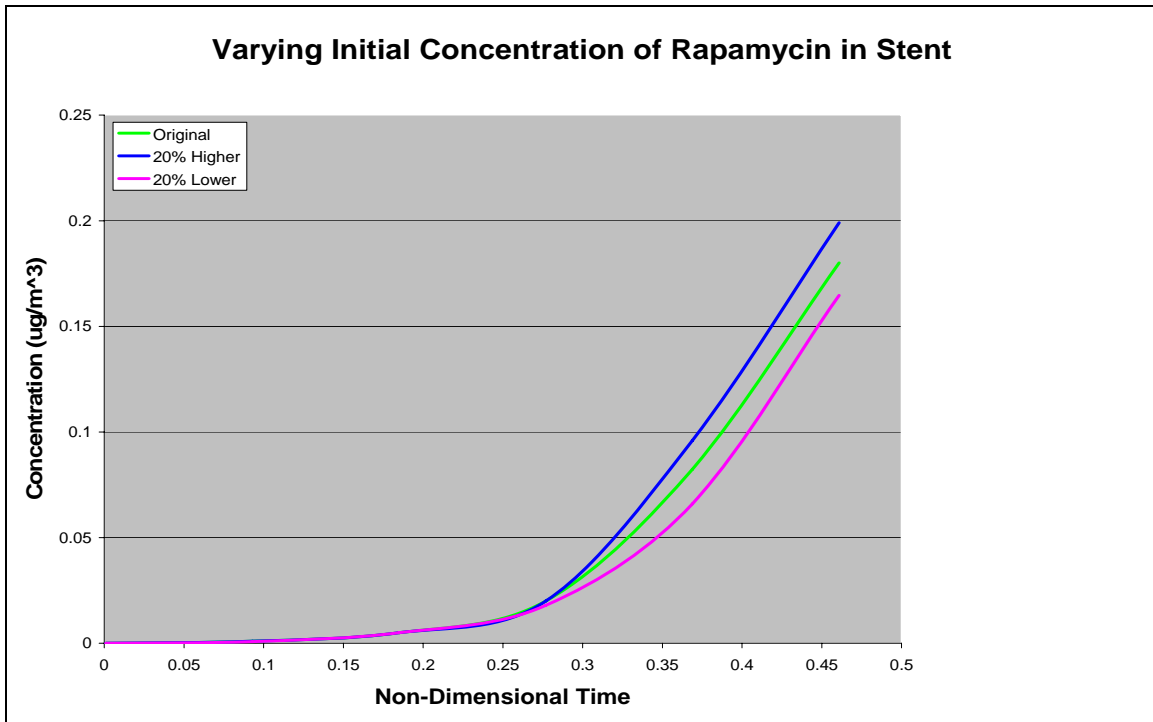


**Figure 3.7:** Plot of concentration versus time for our original initial concentration of Rapamycin in the stent, a concentration 20% higher, and a concentration 20% lower. The final time for the figure is one month, which is why a steady-state concentration is not reached.

### 3.2.2 Variation of Diffusivity of Rapamycin in Intima

Variation of diffusivity of Rapamycin in the intima was our next sensitivity analysis. Diffusivity values were increased and decreased by 20% to test the sensitivity of our model to this parameter, as widely varying diffusivity values for the drug in the intima were found for real-life situations (see Appendix C for further discussion). As shown by figure 3.8, it was found that this parameter had the greatest effect on the final concentration of Rapamycin in the intima, likely because it dictates how far and how much of the drug will travel through the intima in a specified amount of time. A higher diffusivity will result in more drug traveling further, which will result in a greater concentration of drug reaching further into the tissue. Because our design is so sensitive to this parameter, there must be special attention paid to choosing a biologically-accurate diffusivity value for the intima.

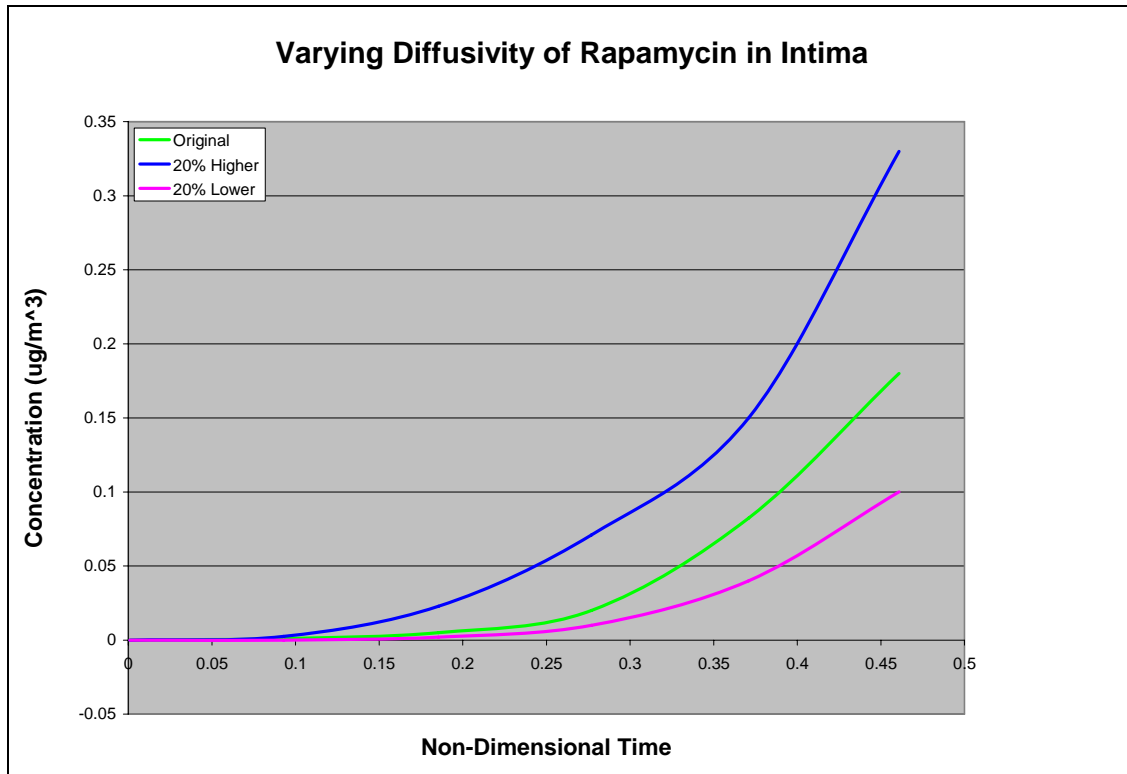


**Figure 3.8:** Plot of concentration versus time for our original diffusivity of Rapamycin in the intima, a diffusivity 20% higher, and a diffusivity 20% lower. The final time for the figure is one month, which is why a steady-state concentration is not reached.

### 3.2.3 Variation of Diffusivity of Rapamycin in Stent

Our final sensitivity analysis was varying the diffusivity of Rapamycin in the stent. We chose to vary this parameter due to the large range of diffusivity values found in various literature references. Additionally, because we chose to model the stent as a homogeneous polymer rather than a polymer-coated metal stent, sensitivity to a range of diffusivity values was a concern. As shown in Figure 3.9, this parameter was the least-sensitive to small changes. This is likely because the stent diffusivity is currently relatively large; small changes will not greatly inhibit drug transfer to the intima. However, as shown in Figure 3.9, higher diffusivities still yield higher drug concentrations in the intima for short times.

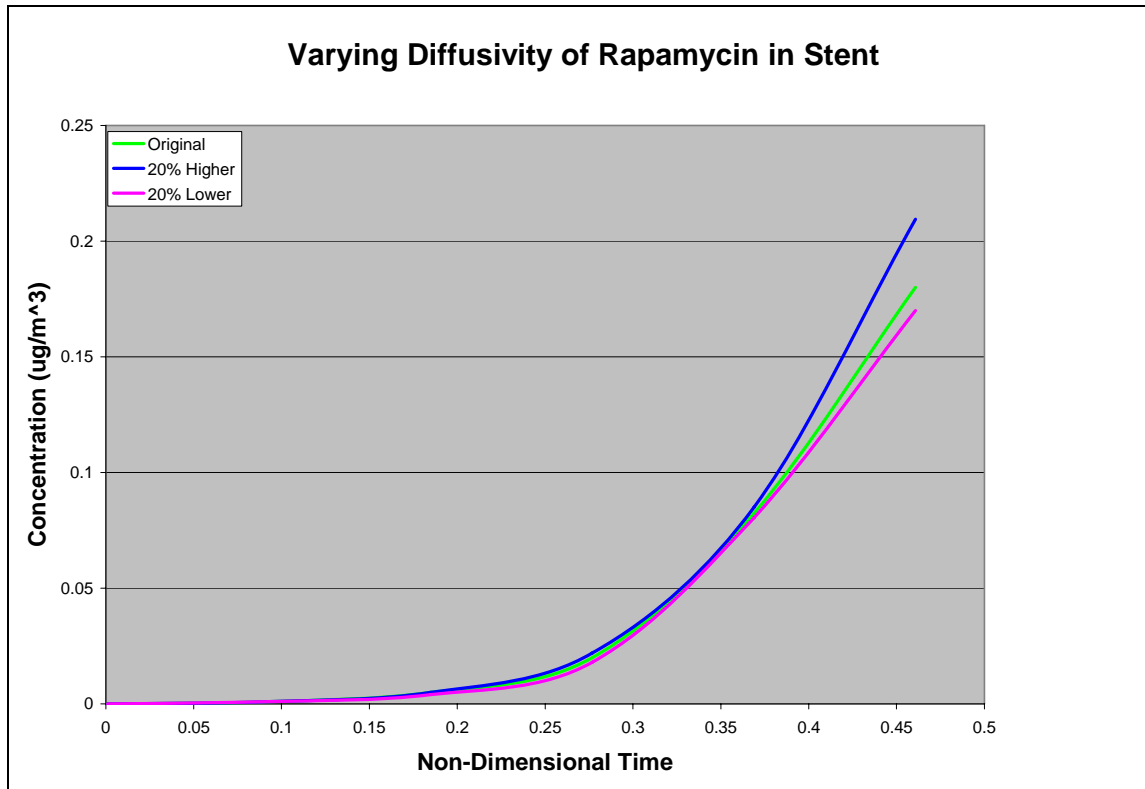


**Figure 3.9:** Plot of concentration versus time for our original diffusivity of Rapamycin in the stent, a diffusivity 20% higher, and a diffusivity 20% lower. The final time for the figure is one month, which is why a steady-state concentration is not reached.

### 3.3 Results vs. Expected Results

For the most part, our results reflected a realistic biological drug-diffusion process as anticipated. The drug diffusion assumed to be radial regardless of the fact that we modeled the stent thickness as a square. The drug concentration at deeper points in the tissue was less than those closer to the stent. The problem also reached steady state after a period of about 9 months, indicating that the drug concentration remains effective during the period of highest risk of restenosis.

However, there were also many unexpected results such as the drug accumulating in areas rather than staying at the same concentration. As seen from Figure 3.2, the drug accumulated around the stent while diffusing outwards. This unexpected result could be due to the fact that we assumed the drug elimination, drug binding, partition coefficients, and pressure gradients in the artery to be negligible. Had we included these parameters, the drug would not have simply accumulated in certain areas, but rather stayed at a steady state concentration, indicating the drug was both diffusing and being eliminated from the area.

Another unexpected result was that initially, it appeared that there was no change in drug concentration at the convective boundary. Simply looking at the contour plots obtained, one would assume that there was no real difference in concentration at the lumen/intima interface. Since our convective coefficient (0.915) is so small, it acts like an insulating boundary condition rather than a convective condition. When zooming into the contour plot, there does appear to be a change of approximately 2% at the periphery of the semicircular concentration gradient.

## [4] Conclusions and Design Recommendations

### 4.1 Conclusion

Using all original parameters, it is concluded that the Rapamycin drug reaches a concentration of  $48 \mu\text{g}/\text{m}^3$  in the entire intima surrounding the stent after nine months. This is within the therapeutic concentration range. The solution is obtained using a drug diffusivity of  $D = 1 \times 10^{-13} \text{ m}^2/\text{s}$ , a tissue diffusivity of  $D = 1 \times 10^{-14} \text{ m}^2/\text{s}$ , and an initial drug concentration of  $c_s = 170 \mu\text{g}/\text{m}^3$ . This concentration will effectively prevent restenosis during the first year after stent deployment, the critical time for which tissue ingrowth and other immune responses are most likely to occur.

### 4.2 Realistic Constraints

When creating our geometry, a number of simplifications were made and must be addressed. The first, and most drastic simplification we made is disregarding the blood velocity in the artery. When we first started, we modeled a velocity profile in the lumen. However, due to small diffusivity values and constraints due to non-dimensionalization, the velocity profile was found to be too complex to implement. Therefore, the fluid flow was replaced by a convective boundary layer at the lumen/intima interface.

Other major simplifications arose from the fact that the arterial geometry, as well as the surrounding heart geometry, is very complex. In the artery itself, there are a total of five different tissue layers, whereas we modeled two tissue layers that incorporated all five. Also, depending on many factors, including age, gender, and body size, the diameter of the artery may vary greatly from person to person. This variation can result in highly variable blood velocities in the artery, which can be translated into different convective terms in our model. Additionally, branching in arteries, which cannot be easily modeled, may affect the blood velocity.

When creating our stent model, we used simplified concentric circles, whereas manufacturing companies utilize much more complex three-dimensional geometries, which could affect the true concentration of Rapamycin in the intima. However, these complex geometries are nearly impossible to duplicate as an axi-symmetric geometry in GAMBIT, and we feel that our simplified model did not produce significant deviation from experimental results, meaning that our geometry simplification was not a major source of error.

Metal is currently the only support material for clinically-approved stents; because of this, the stents must permanently remain in the body. Due to the relatively adolescent nature of drug-eluting stents, long-term effects of a permanent stent in the artery have not been explored in depth. Past permanent implants have resulted in immune responses such as tissue ingrowth into the stent, particulate debris of the stent into the blood and clot formation around the foreign object<sup>8</sup>. These responses can be greatly reduced if the stent were to degrade after prevention of restenosis has been achieved. Biodegradable polymer stents are currently being developed to help solve this problem; these stents will remain in the body as long as it is needed, then safely disintegrate into the blood and surrounding tissues. However, one barrier in using a biodegradable polymer stent is that the polymer is not strong enough to withstand shear forces due to arterial blood flow. Hopefully, in the near future, long-term sustainability can be achieved through a temporary implant. For further elaboration on solution constraints, see Appendix C.

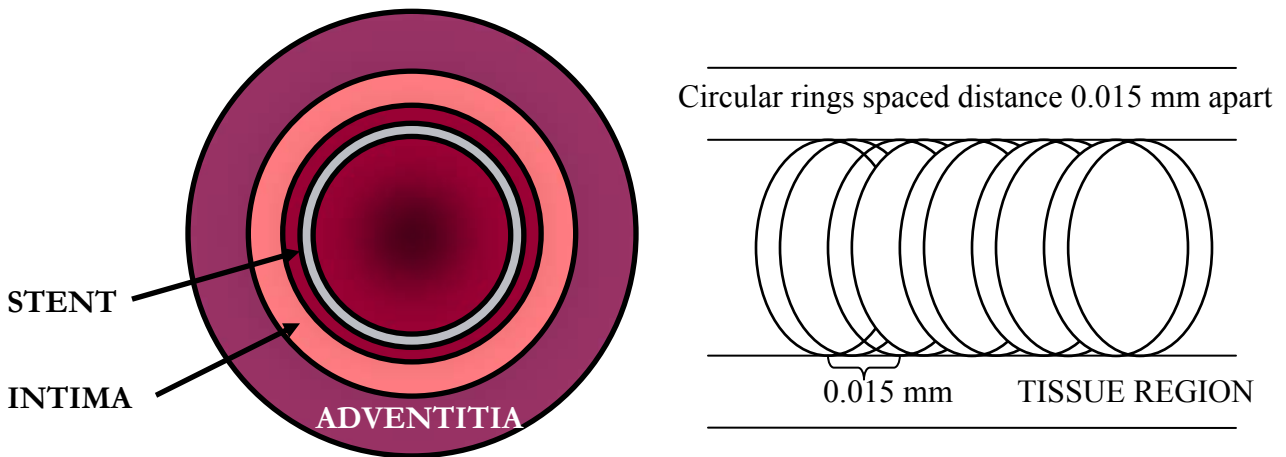
### 4.3 Design Recommendations

We recommend that stents should be designed to hold an initial concentration of  $6 \times 170 \mu\text{g}/\text{m}^3$ , which is  $1020 \mu\text{g}/\text{m}^3$ . This initial concentration has been shown to effectively prevent restenosis during the critical first year of post-implantation. We would advise use of Rapamycin instead of Paclitaxel, due to the potential toxicity of Paclitaxel<sup>5</sup>. For design, we would also recommend a stent composition that would yield lower values of stent diffusivity to provide a better drug distribution in time because the concentration level in the tissue would be higher. Additionally, a slower drug release process may decrease the amount of drug that is lost to blood flow or diffused to deeper tissues that do not need medication.

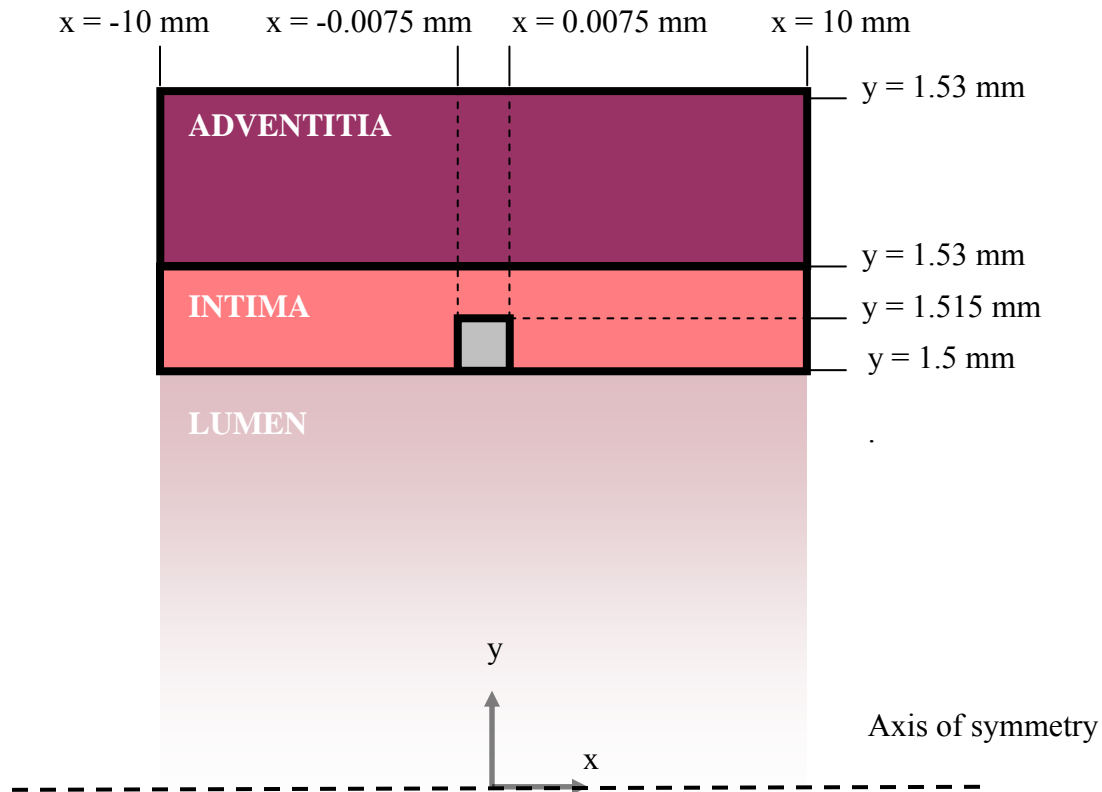
## [5] Appendices

### Appendix A – Mathematical Statement of Problem

#### A.1 Geometry and Schematic



### A.1.1 Geometry



### A.1.2 Governing Equation

Species Equation:

$$\frac{\partial c_d}{\partial t} = D \left( \frac{\partial^2 c_d}{\partial x^2} + \frac{\partial^2 c_d}{\partial y^2} \right)$$

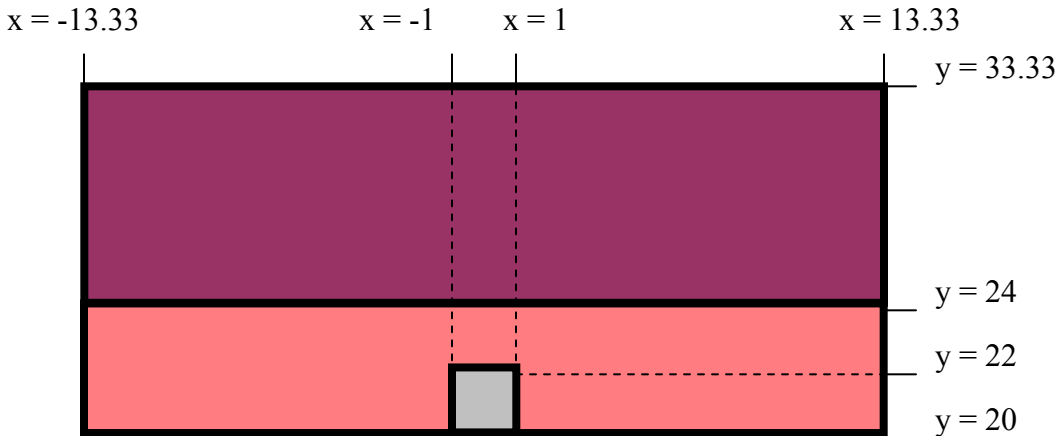
### A.2 Input Parameters

Variable	Value (Dimensional)	Value* (Non-dimensional)
Diffusivity <sub>stent</sub> <sup>7</sup>	$1.0 \times 10^{-13} \text{ m}^2/\text{s}$	10
Diffusivity <sub>adventitia</sub> <sup>10</sup>	$1.0 \times 10^{-14} \text{ m}^2/\text{s}$	1
Diffusivity <sub>intima</sub> <sup>10</sup>	$1.0 \times 10^{-14} \text{ m}^2/\text{s}$	1
Duration of Simulation ( $t_{\text{final}}$ )	$6.31 \times 10^7 \text{ s}$ (2 years)	11.2
Time Step (dt)	1 s	0.5
Mass transfer coefficient ( $h_m$ ) <sup>10</sup>	$1.22 \times 10^{-11} \text{ m/s}$	0.915

## Methods of Non-Dimensionalization

There was a need to non-dimensionalize our parameters and geometry because our values were extremely small. Since Fidap could not handle such small parameters there was a need to non-dimensionalize which allowed us to work on a bigger scale.

- Characteristic Length:  $L = 7.5 * 10^{-6} \text{ m}$



- Stent Diffusivity:  $D_{\text{stent}}^* = \frac{D_{\text{Stent}}}{D_{\text{Adventitia}}} = 10$
- Adventitia Diffusivity:  $D_{\text{advent}}^* = \frac{D_{\text{advent}}}{D_{\text{advent}}} = 1$
- Duration of Simulation:  $(t_{\text{final}})^* = \frac{t_{\text{final}} D_{\text{advent}}}{L^2} = 11.2$
- Mass transfer coefficient:  $h_m^* = \frac{L^* h_m}{D_{\text{advent}}} = 0.915$

## A.3 Initial and Boundary Conditions

### A.3.1 Initial Conditions

$$C_{\text{tissue}0} = 0$$

$$C_{\text{stent}0} = 170 \mu\text{g}/\text{m}^3$$



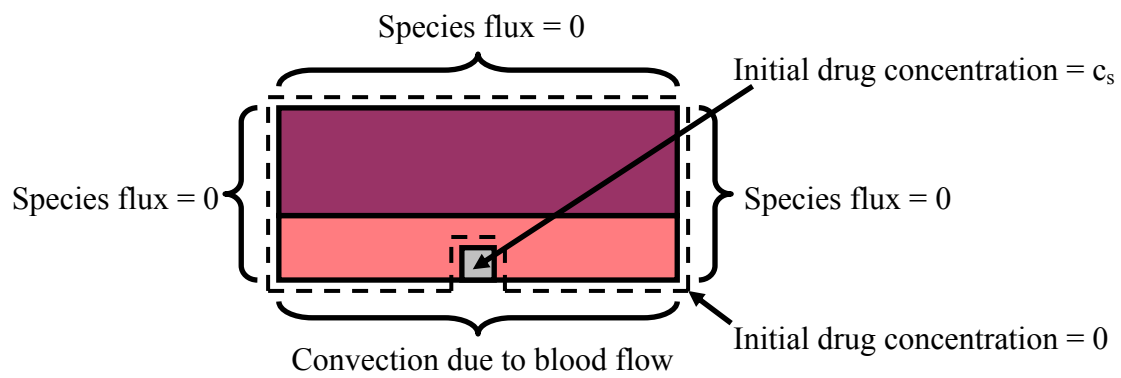
### A.3.2 Boundary Conditions

Lumen-stent/intima interface:  $\frac{\partial c_d}{\partial x} \Big|_{x,y=0} = h_m (c_\infty - c_s)$

$$\frac{\partial c_d}{\partial y} \Big|_{x,y=0} = h_m (c_\infty - c_s)$$

Left, right, and top boundary:  $\frac{\partial c}{\partial x} \Big|_{x,y} = 0$

$$\frac{\partial c}{\partial y} \Big|_{x,y} = 0$$



## Appendix B -- Solution Details

### B.1 Solver Statements

#### B.1.1 PROBLEM Statement

PROB (AXI-, ISOT, NOMO, TRAN, LINE, FIXE, NEWT, INCO, SPEC = 1.0)

<u>Define Models</u>	<u>FIINP</u>	<u>Reason</u>
Geometry Type	Axi-symmetric (AXI-)	Only one calculation was necessary due to our geometry having symmetry about an axis
Temperature Dependence	Isothermal (ISO T)	Problem was independent of temperature
Viscous Dependence	Momentum Turned Off (NOMO)	The blood flow was not modeled, therefore there was not fluid flow in the problem
Time Dependence	Transient (TRAN)	Problem was dependent on time
Deforming Boundary	Fixed (FIXE)	The surface was unchanging
Convective Term	Linear (LINE)	No convection
Fluid Type	Newtonian (NEWT)	There was no fluid flow
Flow Regime	Incompressible (INCO)	Since there was no fluid flow, this term is not relevant
Species Dependence	Species Present (SPEC=1.0)	The mass species present was the drug in the stent

#### B.1.2 SOLUTION Statement

SOLU (S.S. = 50, VELC = 0.100000000000E-02, RESC = 0.100000000000E-01, SCHA = 0.000000000000E+00, ACCF = 0.000000000000E+00)

<b>Commands</b>	<b>FIINP</b>	<b>Reason</b>
Solution Method	Successive substitutions of 50 iterations (S.S.=50)	Default setting
	Velocity Convergence (VELC=0.100E-02)	Default setting
	Result Convergence (RESC=0.100E-01)	Default setting
	Solution Change (SCHA=0.00)	Solution check was disabled
Relaxation Factor	Relaxation Factor (ACCF=0.00)	There was no relaxation factor incorporated in the our problem

**B.1.3 TIME INTEGRATION Statement:**

TIME (BACK, FIXE, TSTA = 0.000000000000E+00, TEND = 0.4608,  
DT = 0.100000000000E-02, NSTE = 5000)

Command	FIINP	Reason
Time Integration	Backward (BACK)	Used for transient analysis
Time Stepping Algorithm	Fixed (FIXE)	Increment of time is unchanging
Starting Time	Start Time (TSTA=0.00)	Starting time is at 0 seconds
End Time	End Time (TEND=0.4608)	Ending time is at 1 month non-dimensionalized
Time Increment	Time Step Size (DT=0.10E-02)	Size of time increment
Number of Time Steps	Number of Time Steps(NSTE=5000)	The maximum number of discrete time integration steps

**B.2 Mesh**

**B.2.1 Plot of Mesh**

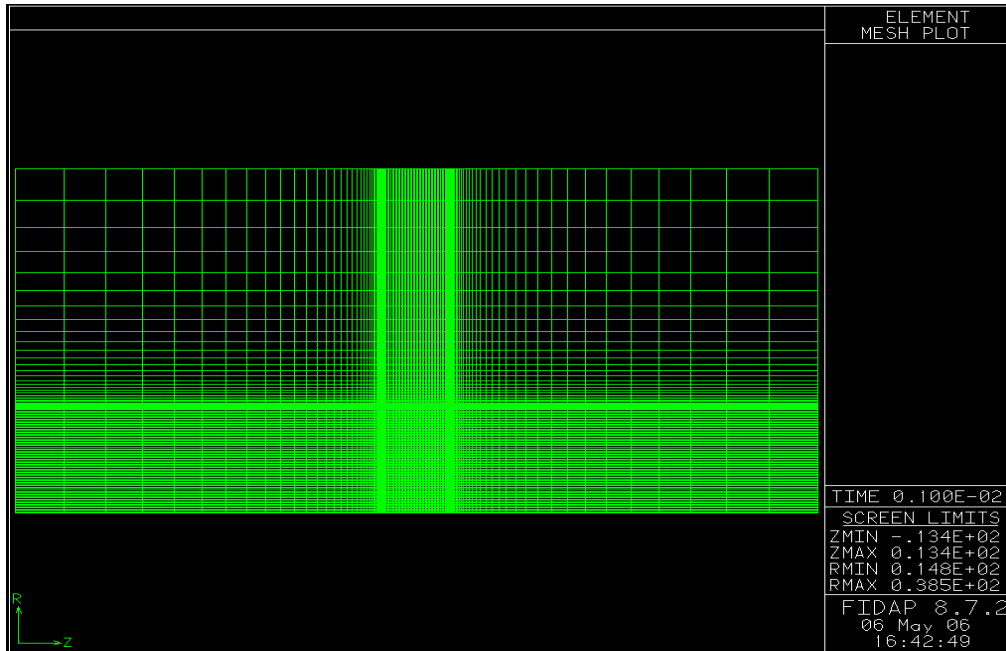


**Figure B1:** A plot of the element mesh, containing 19,000 elements. The mesh density is greater nears the stent, where the greatest change in drug concentration will occur.

### B.2.2 Plot of Node Numbers:

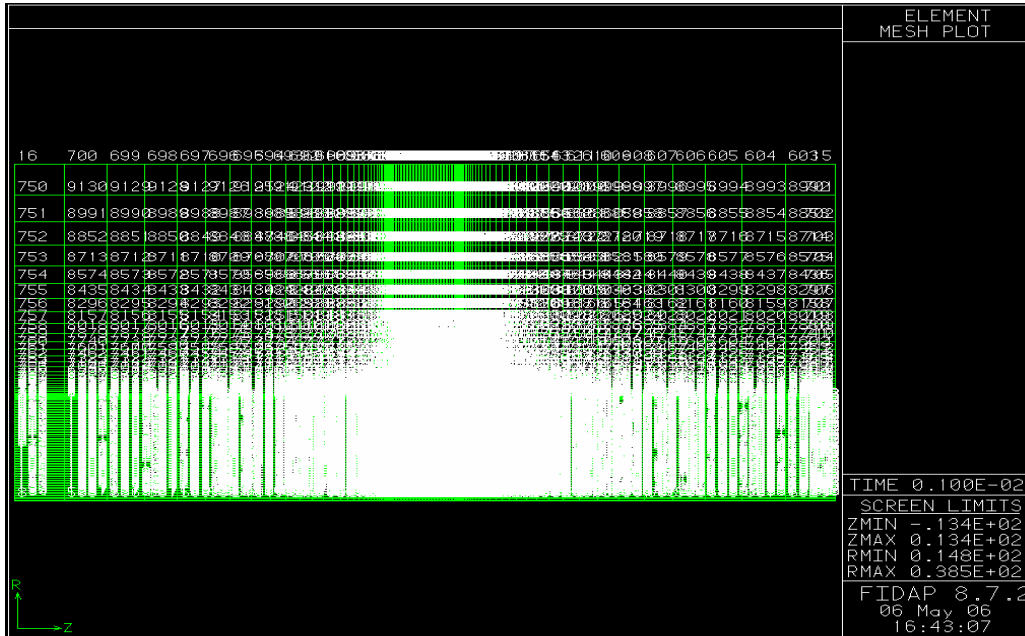
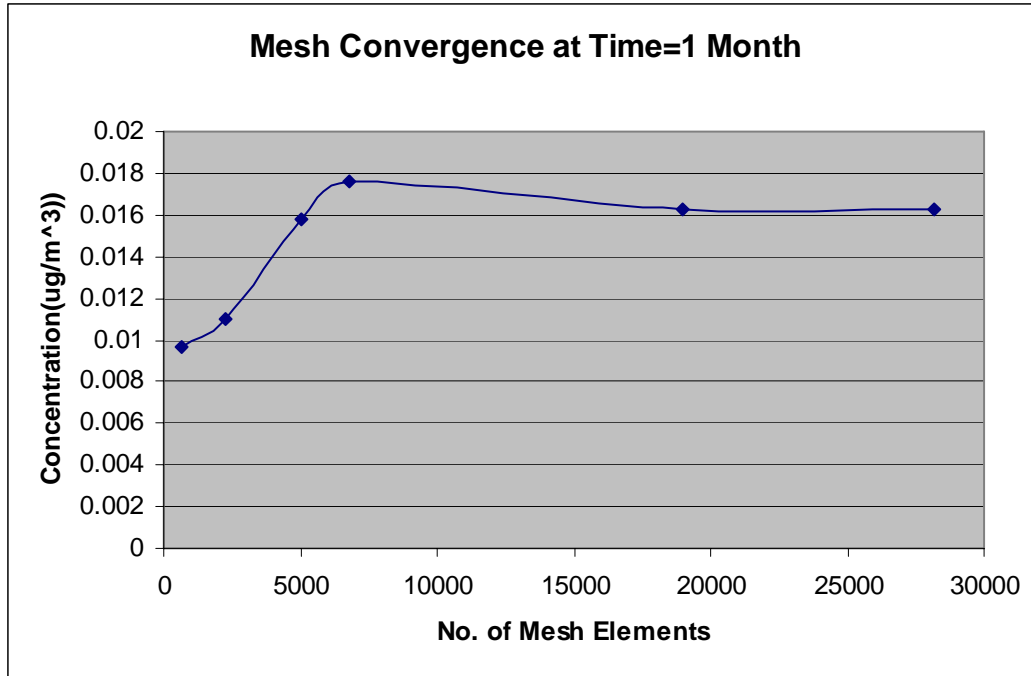


Figure B2: A plot of the element mesh with node numbers labeled.

### B.2.3 Mesh Convergence

To ensure that our mesh converged, we decided to take the drug concentration at a particular node inside the intima at the same time for six different meshes. Our initial mesh was not sufficient, because there was a large difference in concentration at the node for a finer mesh. We continued to refine our mesh until we obtained the same concentration value at a single node for the current and more refined mesh. At 19,000 elements a concentration of about  $0.016\mu\text{g}/\text{mm}^2$  and at a mesh with 28,180 elements, the same concentration value was obtained. Therefore, we considered our mesh to converge at 19,000 elements and then used this refined mesh to solve. Ensuring that our mesh converges results in a solution that is independent of the mesh.



**Figure B3:** Mesh convergence study for six mesh configurations at a single node inside the tissue.

### B.3 FIINP File

```
//FICONV(NEUTRAL,NORESULTS,INPUT)
/ INPUT(FILE= "convect.FDNEUT")
/ END
/ *** of FICONV Conversion Commands
/TITLE
/
/ *** FIPREP Commands ***
/
FIPREP
PROB (AXI-, ISOT, NOMO, TRAN, LINE, FIXE, NEWT, INCO, SPEC = 1.0)
PRES (MIXE = 0.100000000000000E-34, DISC)
EXEC (NEWJ)
SOLU (S.S. = 50, VELC = 0.100000000000000E-02, RESC = 0.100000000000000E-01,
```

```

    SCHA = 0.000000000000E+00, ACCF = 0.000000000000E+00)
TIME (BACK, FIXE, TSTA = 0.000000000000E+00, TEND = 0.4608,
    DT = 0.100000000000E-02, NSTE = 5000)
OPTI (SIDE)
DATA (CONT)
PRIN (NONE)
POST (RESU)
SCAL (VALU = 1.0)
ENTI (NAME = "drugstent", SOLI, PROP = "blood", SPEC = 1.0,
    MDIF = "C1_drugstent")
ENTI (NAME = "adventitia", SOLI, PROP = "mat1", SPEC = 1.0,
    MDIF = "C1_adventitia")
ENTI (NAME = "intima", SOLI, PROP = "mat2", SPEC = 1.0, MDIF = "C1_intima")
ENTI (NAME = "topadventitia", PLOT)
ENTI (NAME = "rightadvent", PLOT)
ENTI (NAME = "leftadvent", PLOT)
ENTI (NAME = "leftint", PLOT)
ENTI (NAME = "rightint", PLOT)
ENTI (NAME = "botstent", ESPE, MSPT = "botstent")
ENTI (NAME = "topstent", PLOT)
ENTI (NAME = "rightstent", PLOT)
ENTI (NAME = "leftstent", PLOT)
ENTI (NAME = "toplumen", ESPE, MSPT = "toplumen")
ENTI (NAME = "topintima", PLOT)
DIFF (SET = "C1_drugstent", CONS = 10.0)
DIFF (SET = "C1_adventitia", CONS = 1.0)
DIFF (SET = "C1_intima", CONS = 1.0)
SPTR (SET = "botstent", CONS = 0.915, REFS = 1.0, POWE = 1.0)
SPTR (SET = "toplumen", CONS = 0.915, REFS = 1.0, POWE = 1.0)
BCFL (SPEC = 1.0, CONS = 0.000000000000E+00, ENTI = "topadventitia")
BCFL (SPEC = 1.0, CONS = 0.000000000000E+00, ENTI = "rightadvent")
BCFL (SPEC = 1.0, CONS = 0.000000000000E+00, ENTI = "leftadvent")
BCFL (SPEC = 1.0, CONS = 0.000000000000E+00, ENTI = "leftint")
BCFL (SPEC = 1.0, CONS = 0.000000000000E+00, ENTI = "rightint")
ICNO (SPEC = 1.0, CONS = 170.0, ENTI = "drugstent")
ICNO (SPEC = 1.0, CONS = 0.000000000000E+00, ENTI = "adventitia")
ICNO (SPEC = 1.0, CONS = 0.000000000000E+00, ENTI = "intima")
EXTR (ON, AFTE = 25, EVER = 15, ORDE = 2, NOKE, NOFR)
END
/ *** of FIPREP Commands
CREATE(FIPREP,DELE)
CREATE(FISOLV)
PARAMETER(LIST)

```

## Appendix C – Sensitivity of Rapamycin Concentration in Intima to Real-World Parameters

Because a very large range of parameter values can be found for currently manufactured and clinically-tested drug-eluting stents, in addition to our sensitivity analysis, we performed further comparison analysis to show the effect of using a larger range of initial concentrations, different anti-restinosis drugs, and binding patterns in the arterial wall.

Highly Variable Parameters	Range in Literature	Value Used in Solution
1. Initial Concentration of Rapamycin Immobilized in Stent <sup>7</sup>	Low <sup>4</sup> : 5 $\mu\text{g}/\text{m}^3$ High <sup>1</sup> : 196 $\mu\text{g}/\text{m}^3$	170 $\mu\text{g}/\text{m}^3$
2. Diffusion of Rapamycin through Intima (due to drug type and tissue binding) <sup>10</sup>	Low <sup>3</sup> : $1.0 \times 10^{-13} \text{ m}^2/\text{s}$ High <sup>3</sup> : $4.87 \times 10^{-12} \text{ m}^2/\text{s}$	$1.0 \times 10^{-14} \text{ m}^2/\text{s}$
3. Stent diffusivity <sup>10</sup>	Low <sup>1</sup> : $1.0 \times 10^{-16} \text{ m}^2/\text{s}$ High <sup>1</sup> : $1.0 \times 10^{-10} \text{ m}^2/\text{s}$	$1.0 \times 10^{-13} \text{ m}^2/\text{s}$

**Table C.1:** Variation in parameters affecting steady-state Rapamycin concentration in the intima

### C.1 Influence of Initial Concentration of Rapamycin Immobilized in Stent

Figure C.1 illustrates the significant difference in Rapamycin concentration profiles in the intima. While each initial concentration reaches a steady-state concentration after approximately the same time interval, the higher concentrations reach a therapeutic concentration more rapidly, but have a higher risk of reaching toxic levels. While small variations in initial drug concentration, as shown by the initial sensitivity analysis, did not greatly affect concentration profiles, considerable changes were found for the large variance found in studies of drug-elution from Rapamycin-coated stents.

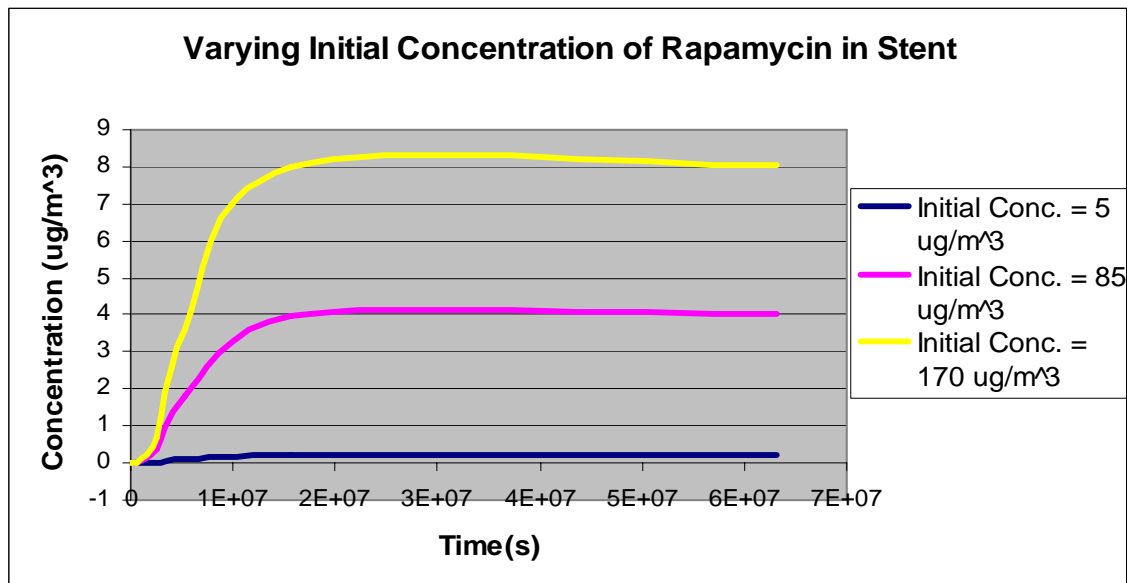


**Figure C.1.** Plot of concentration versus time for three widely different initial concentrations found in published drug-eluting stent literature for a two-year simulation period.

## C.2 Influence of Drug Diffusivity in Arterial Tissue

Drug diffusivity through the intima was an extremely variable parameter in this simulation, and experiment data suggests drug type and tissue-binding effects greatly affect the effective drug diffusivity.

### C.2.1 Drug Type Effects on Diffusivity

Two major drugs are currently utilized in drug-eluting stents: Paclitaxel and Rapamycin. Both compounds have similar molecular masses (1 kDa), solubilities of 6 g/mL, and are both hydrophobic<sup>5</sup>, leading to similar elution profiles. However, due to the slight differences in molecular weight and hydrophobicity, Paclitaxel and Rapamycin have slightly different diffusivities in tissue. As shown by Figure C.2.1, change in diffusivity based on the differences found between Paclitaxel and Rapamycin had virtually no effect on the solution. Therefore, any error in diffusivity values due to approximating Paclitaxel data as Rapamycin data would result in a similar drug concentration at a particular tissue depth.

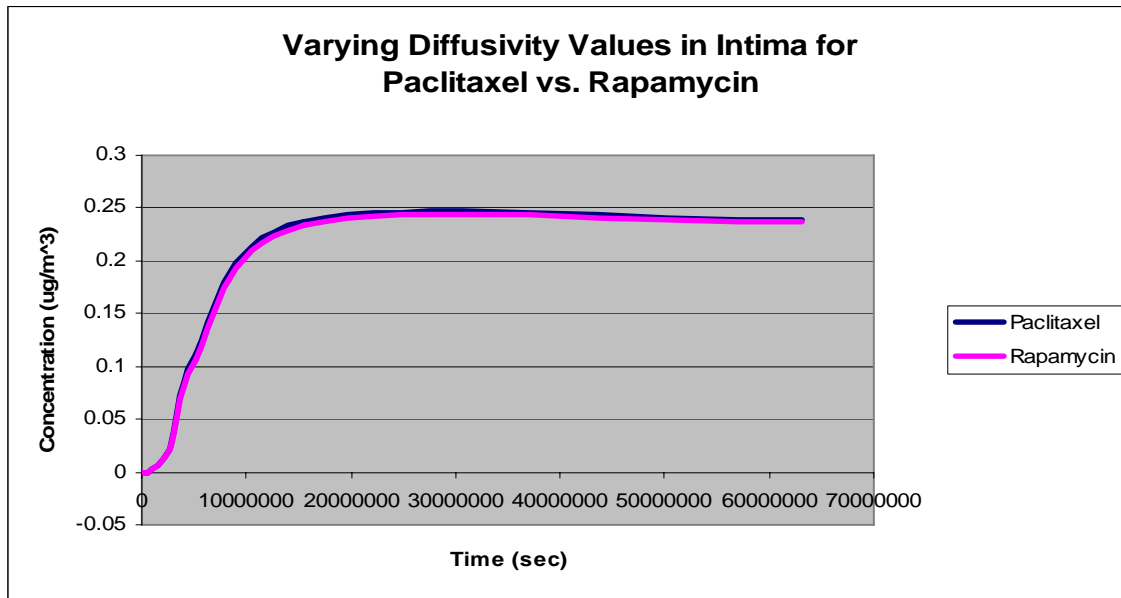


**Figure C.2.1.** Plot of concentration versus time for Rapamycin (our original solution) and Paclitaxel, a similar anti-restinosis drug, for a two-year simulation period.

### C.2.2 Tissue Binding Effects on Diffusivity

Specific binding to intracellular receptors in the intima differs greatly between Rapamycin and Paclitaxel, creating dissimilarities between the accumulation of Paclitaxel and Rapamycin in distinct areas of the vascular wall. Optimally, drug concentrations should peak in the intimal layer of the vascular wall<sup>2</sup>. While Rapamycin distributes equally within the vascular layers, Paclitaxel accumulates in the adventitia, potentially because Paclitaxel has specificity to microtubules, while Rapamycin shows similar specific binding to FKBP12, which have different tissue distributions in the coronary artery<sup>5</sup>. A partition coefficient  $k \gg 1$  has been found for Paclitaxel<sup>3</sup>; however, we were unable to implement this due to limitations inherent in FiDAP.



Studies have shown that Paclitaxel partitions significantly in the adventitia, while Rapamycin is more evenly distributed throughout the arterial wall. This is a major point of concern for clinical implementation, as uneven binding of Paclitaxel could lead to toxic effects due to abnormally high concentrations in the tissue.

### C.3 Stent Composition Effects on Diffusivity of Rapamycin in Stent

Because many different polymer types are used in drug-eluting stents, it was important to consider the variation in diffusivity of the stent. Due to constraints arising from a lack of fluid flow and differing stent compositions, an optimal solution would be creation of a varying boundary condition at the surface of the stent, based on experimental data. This would most accurately mimic the true elution profile; however, no literature values could be found for the such a profile for the full 2 year simulation time period.

As an alternative to modeling a metallic stent with a surface polymer coating, we determined that simulation of a biodegradable, polymeric stent was optimal for solution in FiDAP. These nonpermanent stent have the potential to remain in situ for a predicted period of time, and because there is a decreasing need for a permanent prosthesis after 6 months<sup>1</sup>, polymeric stents are an optimal solution to restinosis. Two polymers commonly used in Rapamycin-eluting stents are polyethylenevinylacetate (PEVA) and polybutylmethacrylate (PBMA).<sup>7</sup> Two other polymers currently under clinical investigation are polylactide (PLA) and poly(lactide-co-glycolide) (PLG).

<b>Drug</b>	<b>Diffusion (cm<sup>2</sup>/s) from PLA Stent<sup>1</sup></b>	<b>Diffusion (cm<sup>2</sup>/s) from PLG Stent<sup>1</sup></b>
Paclitaxel	4.9 x 10 <sup>-12</sup>	5.7 x 10 <sup>-9</sup>
Rapamycin	3.1 x 10 <sup>-12</sup>	4.5 x 10 <sup>-11</sup>

**Table C.3:** Different drug diffusivities depending on polymer type.

The relatively wide range of diffusivity values found simply by modifying the type of polymer demonstrates the complexity of choosing appropriate diffusivity values; the nature of the polymer in which Rapamycin is immobilized should be a concern for future modeling and design of drug-eluting stents.

## Appendix D - References

- <sup>1</sup>Alexis, F., Venkatraman, S.S., Rath, S.K., Boey, F. 2004. *In vitro study of release mechanisms of Paclitaxel and Rapamycin from drug-incorporated biodegradable stent matrices. Journal of Controlled Release* 98:67-74.
- <sup>2</sup>Costa, M.A., Simon, D.I. 2005. *Molecular Basis of Restenosis and Drug-Eluting Stents. Circulation* 111:2257-2273.
- <sup>3</sup>Creel, C.J., Lovich, M.A., Edelman, E.R. 2000. *Arterial Paclitaxel Distribution and Deposition. Circulation Research*. 86:879-884.
- <sup>4</sup>Hwang, C., Wu, D., Edelman, E.R. 2001. *Physiological Transport Forces Govern Drug Distribution for Stent-Based Delivery. Circulation* 104:600-605.
- <sup>5</sup>Levin, A.D., Vukmirovic, N., Hwang, C., Edelman, E.R. 2004. *Specific binding to intracellular proteins determines arterial transport properties for Rapamycin and paclitaxel. PNAS* 101:9463-9467.
- <sup>6</sup>Mongrain, R., Nulman-Fleming, N., Bertrand, O. June 25, 2003. *3D numerical simulations of stent-based local drug delivery using realistic stent and vascular wall structures. 2003 Summer Bioengineering Conference, Key Biscayne, Florida.*
- <sup>7</sup>Serruys, P.W., Regar, E., Carter, A.J. 2002. *Rapamycin eluting stent: the onset of a new interventional cardiology. Heart* 87:305-307.
- <sup>8</sup>Wessely, R., Schomig, A., Kastrati, A. 2006. *Sirolimus and Paclitaxel on Polymer-Based Drug-Eluting Stents: Similar But Different. Journal of the American College of Cardiology* 47:708-714.
- <sup>9</sup>Wieneke, H., Dirsch, O., Sawitowski, T., Li Gu, Y., Brauer, H., Dahmen, U., Fischer, A., Wnendt, S., Erbel, R. Oct 15, 2003. *Synergistic effects of a novel nanoporous stent coating and tacrolimus on intima proliferation in rabbits. Catheterization and Cardiovascular Interventions* 60:399-407.
- <sup>10</sup>Zunino, P. 2004. *Multidimensional Pharmacokinetic Models Applied to the Design of Drug-Eluting Stents. Cardiovascular Engineering* 4:181-191.